Article

A High-efficiency Cathode Using Co_3O_4 and Carbon Paper by Electrodeposition for Rechargeable Lithium-oxygen Batteries

Jing Chen [1,†], Tiedong Liu [1,†], Bin Zhang [1,*], Yu Min [2], Hongqiang Wang [3], Qing-yu Li [3,*]

[1] Electronic and Electrical Inspection Division, Shenzhen Academy of Metrology & Quality Inspection, Shenzhen 518060, China; 18684834246@163.com (J.C.); liutiedong71@163.com (T.L.)

[2] Guangdong Research Center for Interfacial Engineering of Functional Materials, Shenzhen University, Shenzhen 518060, China; 812392551@qq.com (Y.M.)

[3] Guangxi Key Laboratory of Low Carbon Energy Materials, School of Chemical and Pharmaceutical Sciences, Guangxi Normal University, Guilin 541004, China; whq72@126.com (H.W.)

* Corresponding author. E-mail: cunzhang93@163.com (B.Z.); liqingyu62@126.com (Q.L.)

† These authors contributed to the work equally and should be regarded as co-first authors.

ABSTRACT: The conductivity, microstructure, low cost, eco-friendliness, simple and controllable preparation are key points of the preparation and application of cathode materials for lithium-oxygen batteries. Considering the above-mentioned important factors comprehensively, the Co_3O_4@CP electrode with a three-dimensional structure was prepared by directly growing Co_3O_4 on the surface of carbon paper (CP) using a simple and controllable electrodeposition method. The obtained Co_3O_4 depositing layer has a nanosheet microstructure and can provide abundant catalytic active sites for the oxygen evolution and reduction reactions. The network architecture of electronic transmission is constructed by CP in the cathode, promoting the efficiency of the electrode reaction. It's worth noting that the binder-free and conductive additive-free cathode is beneficial to reduce side reactions. The lithium-oxygen battery assembled with the obtained Co_3O_4@CP electrode showed satisfactory electrochemical performance. The cell assembled with the obtained Co_3O_4@CP electrode provided a discharge specific capacity of 10954.7 mA·h·g⁻¹ at a current density of 200 mA·g⁻¹, and the voltage profiles of the cell were good under 100 mA·g⁻¹ at a limited capacity of 500 mA·h g⁻¹ based on the mass of Co_3O_4. Therefore, the Co_3O_4@CP composite material is a promising candidate with good application prospects as a cathode material for lithium-oxygen batteries.

Keywords: Co_3O_4; Carbon paper; Catalytic active sites; Electrochemical performance; Lithium-oxygen batteries

1. Introduction

The capacity of state-of-the-art lithium-ion batteries cannot meet the rising demand for the capacity of energy storage equipment [1,2]. In recent years, there has been a sense of urgency in developing next-generation batteries with higher energy density. Among various types of batteries, the lithium-oxygen battery has attracted the most attention from researchers worldwide due to its high theoretical energy density of more than 10,000 W·h·kg⁻¹. This is comparable to the energy density of gasoline, which is 13,000 W·h·kg⁻¹ [3,4]. However, the lithium-oxygen battery system is still in its infancy stage, and many problems need to be paid more attention to, such as how to effectively enhance the discharge capacity and energy efficiency of the rechargeable lithium-oxygen battery system [5]. As an indispensable component of batteries, the microstructure and properties of the cathodes directly affect the performance of the lithium-oxygen whole battery system. This includes the overpotential, discharge efficiency, cycle stability, and so on [6]. In cathode, the electrochemical reaction of $2Li^+ + 2e^- + O_2 \rightleftharpoons Li_2O_2$ ($E_0 = 2.96$ V vs. Li/Li^+) continuously occurs when the lithium-oxygen battery system works. The solid insulating discharge product (Li_2O_2) can block the channels of oxygen permeation in the electrode, causing slow reaction rate during charging, and resulting in a large charge overpotential for the lithium-oxygen battery. Hence, designing a microstructure and components of the cathode, which is beneficial to alleviate the negative effects from Li_2O_2, is all-important [7].

In the process of fabricating traditional cathode of lithium-oxygen battery, binders and conductive additives are usually added in the slurry. Whereas in most cases, binders and conductive additives will have a side reaction with the electrolyte, damaging the catalytic efficiency of the cathode. Using an in-situ synthesis method to construct an original cathode without binders and conductive additives facilitates interfacial electron transfer and enhances the speed of electrochemical reactions in the cathode by enabling direct contact between catalysts and the substrate collector [8]. As is well-known, there are various methods to carry out in-situ synthesis, including hydrothermal method, chemical deposition method, electrodeposition method, etc. Among these methods, electrodeposition is preferred because it is easy to operate and can be implemented at room temperature.

Active catalysts in the cathode play a vital role in improving the efficiency of the lithium-oxygen battery. However, the cost of catalysts has been an obstacle to the widespread application of lithium-oxygen batteries. As a result, some Co-based oxides (e.g., Co_3O_4, CoO) without noble metals have attracted more attention from researchers because of their advantages in terms of price [9–12]. A lot of work related to Co_3O_4 has been implemented, including preparation and application. On the one hand, three-dimensional porous structures of Co_3O_4 have been fabricated via hydrothermal, chemical vapor deposition, or electrodeposition [13]. On the other hand, Co_3O_4-based electrodes for lithium-oxygen batteries have been fabricated using traditional slurry-coating technology [14–16]. Pu Z. et al. demonstrated that Co_3O_4 can be uniformly deposited on the surface of the basal body [17]. Zhao G. Y. et al. showed that the induction of organic binders in the cathode accelerates the degradation process of battery capacity [18]. To sum up, the existing research results have revealed that Co_3O_4 has good comprehensive performance in terms of first discharge capacity and cyclic capacity retention [19–21]. Furthermore, Co_3O_4 as electrode material has been applied to lithium-ion batteries, supercapacitors, and so forth [22].

In this work, a free-standing cathode was prepared using Co_3O_4 and carbon paper by electrodeposition for a rechargeable lithium-oxygen battery, aiming to overcome problems including large charge overpotential, low conductivity, side reactions, etc. The schematic diagram of the synthesized course of the Co_3O_4@CP composite cathode is presented in Figure 1. The obtained Co_3O_4@CP composite cathode mainly illustrates two merits as follows: first, the original pores of the Co_3O_4 can remain in good condition, not being clogged by the binder; second, the Co_3O_4 crystallizes into super-thin nanosheets, which self-assemble into morphology with hierarchical mesopores, bringing forth larger specific surface area and more active sites for the reaction in the cathode.
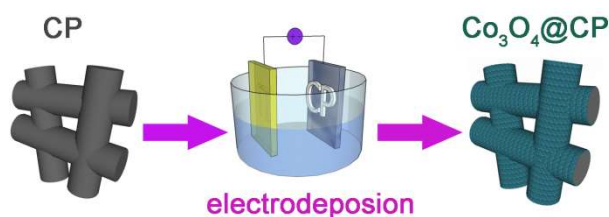
Figure 1. Fabrication process of Co₃O₄@CP composites electrode.

2. Materials and Methods

2.1. Synthesis of Co₃O₄@CP Composites

The reagents (AR) used in this work were all purchased from Shanghai Aladdin Biochemical Technology Co., Ltd. (Shanghai, China). All reagents were used as received without further purification. The Co_3O_4 was uniformly deposited on the CP substrate. The electrodeposition experiment was implemented in 0.1 M $CoSO_4$ at a current density of about 20 mA·cm^{-2} for 4 min. After deposition, the as-produced sample was washed with deionized water several times to neutralize it and dried at 80 °C for 4 h. The dry sample underwent a process of deadburn at 350 °C for 1 h in the atmosphere. The obtained composite after deadburn is marked as Co_3O_4@CP. The load amount of Co_3O_4 in the Co_3O_4@CP sample was measured by the mass difference before and after electrodeposition.

2.2. Characterization

Morphologies analyses were done by making use of Field Emission Scanning Electron Microscope (FEI Quanta 200 FEG, Eindhoven, The Netherlands) and transmission electron microscope (FEI TECNAI G2 12, Eindhoven, The Netherlands). The characterization for phase structure and element composition was implemented by X-ray powder diffraction (D/max 2500 v/pc diffractometer, Rigaku, Tokyo, Japan). The element composition analysis of the Co_3O_4@CP composites was conducted via energy-dispersive X-ray spectroscopy. The chemical states of the Co_3O_4@CP composite were investigated using X-ray photoelectron spectroscopy (Physical Electronics 5400 ESCA, Chanhassen, MN, USA).

### 2.3. Electrochemical Measurement

The Co$_3$O$_4$@CP composite and lithium foil were as the cathode and anode of the lithium oxygen battery, respectively. The diameters of the Co$_3$O$_4$@CP cathode and lithium foil were separately controlled at 14 mm and 15 mm. A piece of Whatman GF/D (Metersbonwe, UK) glass microfiber filter paper was used as the separator between cathode and anode aiming to avert short circuit, and 1.0 M lithium bis(trifluoromethanesulfonyl)imide (LiTFSI) in tetraethylene glycol dimethyl ether as the electrolyte. The whole process of assembling cell was performed in glove box system filled with argon, and the battery was placed in the glove box for more than 12 h. The cells after aging were purged with tetraglyme-saturated oxygen for 2 h before electrochemical tests.

A battery discharge-charge test system (LAND CT2001A) was used to validate the rechargeability at diversified rates at room temperature, and the voltage window was controlled between 2.2 and 4.3 V (vs. Li$^+$/Li). The specific capacity of the cell was measured based on the mass of Co$_3$O$_4$ if it's not explicitly stated. Cyclic voltammetry (CV) was done by IM6 (Kronach, Germany), and the scanning frequency is 0.1 mV·s^{-1}, and the voltage range to be scanned is 2.0~4.5 V. The electrochemical impedance spectroscopy (EIS) test was also implemented via IM6 (Kronach, Germany), and the test parameters were set as follows: frequency range was 100 kHz~10 mHz; voltage amplitude was 5 mV.

3. Results and Discussion

The micro-morphology of the Co$_3$O$_4$@CP cathode material obtained by the process shown in Figure 1 was observed using scanning electron microscopy, as shown in Figure 2. The CP provided an interconnected fibrous network for the electrodeposition of Co$_3$O$_4$, which was evident from the micro-morphology of the Co$_3$O$_4$@CP cathode material that maintained the fibrous network structure after electrodeposition, as seen in Figure 2a,b. Figure 2b shows that the surface of the Co$_3$O$_4$@CP fiber is uniform without noticeable depressions. Figure 2c clearly demonstrates that the Co$_3$O$_4$ was evenly deposited on the surface of the CP fiber, with a thickness of around 100 nm and direct attachment to the fiber surface. Figure 2d is a partial enlargement of the Co$_3$O$_4$ layer, revealing that it is composed of agglomerates of nanosheets and has a porous structure at the micro scale. Overall, the scanning electron microscope (SEM) results demonstrate that the manufacturing process of the Co$_3$O$_4$@CP cathode material shown in Figure 1 was carried out perfectly.
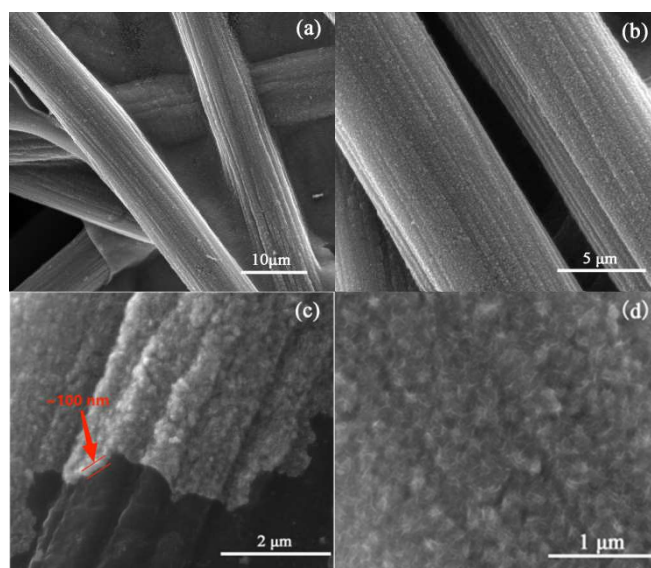
**Figure 2.** (**a**) SEM of the Co$_3$O$_4$@CP composite; (**b**,**d**) the enlarge images of (**a**); (**c**) the Co$_3$O$_4$ layer.

For the purpose of further understanding the micro morphology of the Co$_3$O$_4$ layer on the surface of CP, a part of the Co$_3$O$_4$ layer was exfoliated and characterized via transmission electron microscope (TEM). From Figure 3a, it can be seen that the Co$_3$O$_4$ layer appears in the form of particle aggregates, which is consistent with the SEM result. Additionally, the particles were surrounded by numerous nanosheets, which were connected via the intertwining of these nanosheets without a binder. The interpenetrating structure of the nanosheets, with a thickness of around 4–7 nm, is conducive to forming a hierarchical mesoporous structure, which promotes the diffusion of oxygen and electrolyte in the cathode. Importantly, this kind of interpenetrating nanosheets can provide favorable conditions for the continuous transport of electrons and ions in the cathode simultaneously, thereby improving the efficiency of the electrochemical reaction in the electrode. Figure 2b shows a partial enlargement of Figure 2a, where the nanosheet is thin and transparent like a cicada wing. The high-resolution TEM result (in Figure 3c) shows lattice fringes with a distance of 0.24 nm and 0.28 nm, which agrees with the spacing of the (311) and (220) plane of Co$_3$O$_4$ (JCPDS 65-3103).

To confirm the crystal structure of the Co_3O_4@CP composite, an X-ray diffraction (XRD) test was performed, and the results are presented in Figure S2. Comparing the diffraction spectra of the CP and the Co_3O_4@CP composite, a diffraction peak at around 36.9° in the latter emerges, which is related to the crystal structure of the spinel Co_3O_4 phase assigned to the (311) plane. The characterization results of XRD are consistent with those of TEM.

In order to further verify the uniformity of Co_3O_4 deposition on carbon paper, an energy dispersive spectroscopy (EDS) test was performed, as shown in Figure 4. The Co_3O_4@CP cathode material should consist of Co, O, and C. The results of the EDS test proved that the Co_3O_4@CP cathode material mainly contains the elements of Co, O, and C. In Figure 4, it is clearly seen that the elements of Co, O, and C are evenly distributed in the test sample, which is consistent with the micro-distributing morphology of the Co_3O_4 layer on the CP obtained from the SEM results.
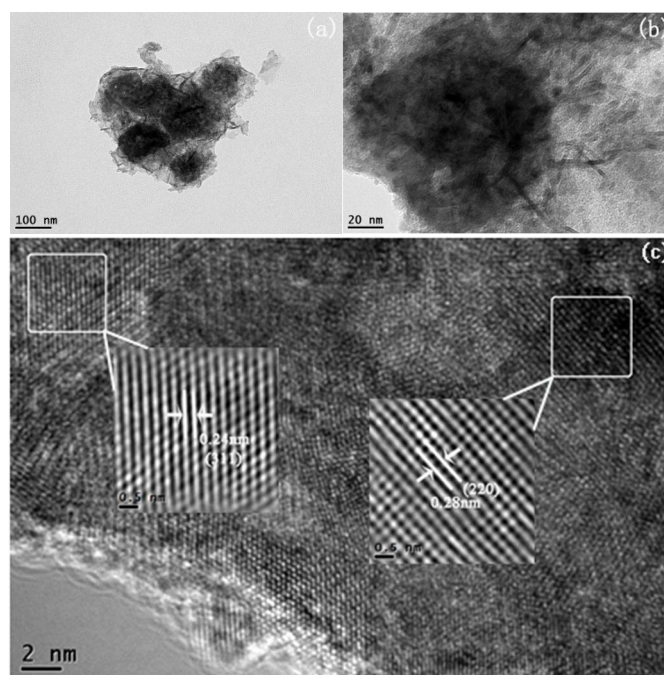

**Figure 3.** (**a,b**) TEM image of the Co_3O_4 depositing layer; (**c**) HRTEM image of the Co_3O_4 depositing layer.
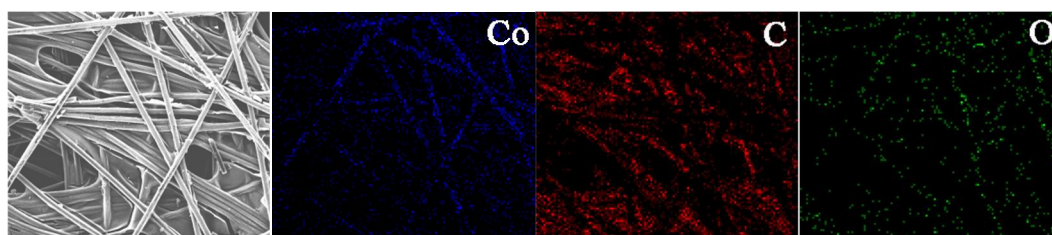
Figure 4. EDS maps of the elements of Co, C, O in the Co_3O_4@CP material.

The chemical state of the elements Co, O, and C in the Co_3O_4@CP cathode material was analyzed through X-ray photoelectron spectroscopy (XPS), as shown in Figure 5. The Co2p, C1s, and O1s peaks were scanned in the XPS map using the XPS peak version 4.1 software for analysis. The Co_3O_4 peaks exhibited two spin-orbital doublets of Co^{2+} and Co^{3+} and two shakeup satellites. The peaks at 779.8 and 795 eV were attributed to Co^{2+}, while the peaks at 778.4 and 794 eV were characteristic peaks of Co^{3+}. Figure 5c displays the peak spectra of O1s, where the two peaks located at 530.2 and 528.9 eV were primarily caused by the O1s binding energy in Co–O and O–H. In Figure 5d, the C1s binding energy of (C–O), (C–H), (C–C, diamond), and (C–C, graphite) resulted in the appearance of four peaks located at 286.4, 284.0, 283.5, and 283.3 eV.
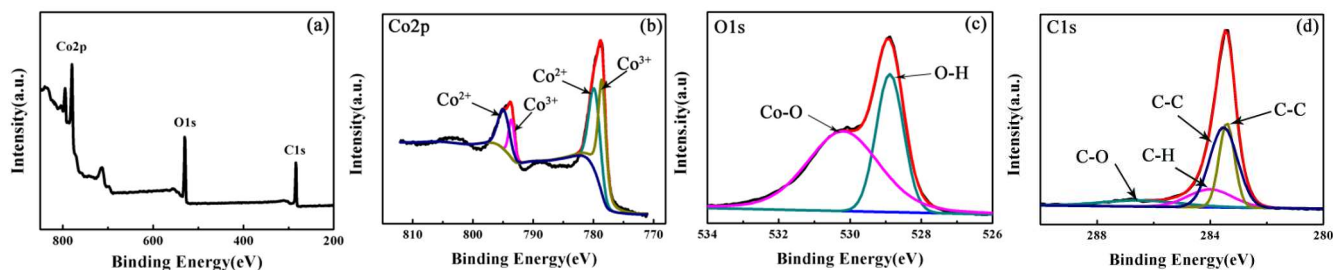
Figure 5. XPS of Co$_3$O$_4$@CP composite. (**a**) Survey scan. (**b**) Co2p spectrum. (**c**) O1s spectrum. (**d**) C1s spectrum.

Subsequently, the electrochemical performances of the cells with Co$_3$O$_4$@CP electrode were preliminarily investigated, which was a straightforward way to assess the properties of Co$_3$O$_4$@CP in a lithium-oxygen battery. The discharge performances of the cell at 200 mA·g^{-1}, 300 mA·g^{-1}, and 500 mA·g^{-1} were shown in Figure 6a. The discharge specific capacity of the cell with Co$_3$O$_4$@CP electrode was up to 10954.7 mA·h·g^{-1} at 200 mA·g^{-1} from 4.3 V to 2.2 V, which was attributed to the good diffusion of oxygen and electrolyte as well as the unimpeded transport of electrons and ions in the Co$_3$O$_4$@CP electrode. When the current density was increased to 500 mA·g^{-1}, the discharge specific capacity of the cell delivered 3407 mA·h·g^{-1}. The cycling charge/discharge of the cell was conducted at a current density of 300 mA·g^{-1} between 2.2 and 4.3 V, as presented in Figure 6b. The discharge specific capacity of the 1st cycle was 7061.5 mA·h·g^{-1}. Unfortunately, the value in the 5th cycle decayed to about 2585.3 mA·h·g^{-1} because of the influence of the side-products in the electrochemical reaction. What is hopeful, however, is that the cycling stability was relatively good after the 5th cycle. In Figure 6c, the cell assembled with Co$_3$O$_4$@CP electrode still could run 50 cycles at a cutoff capacity of 500 mA·h·g^{-1} and a current density of 100 mA·g^{-1}, indicating the satisfactory stability of the voltage plateau. In contrast to traditional cathodes fabricated by the slurry method, the Co$_3$O$_4$@CP electrode omitted the binder and alleviated the obstacle to electron transport. As a consequence, the results obtained here will hopefully encourage further studies on the Co$_3$O$_4$@CP electrode for a lithium-oxygen battery.
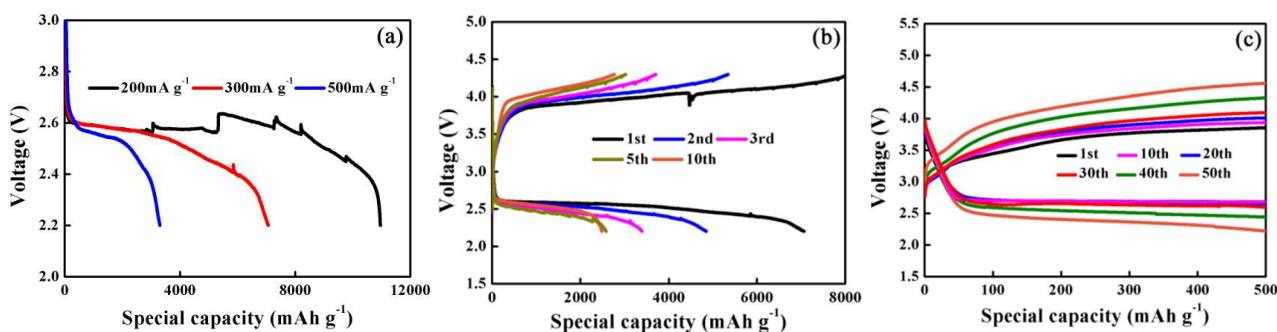
**Figure 6.** (**a**) discharge profiles of Co$_3$O$_4$@CP electrode at 200 mA·g^{-1}, 300 mA·g^{-1} and 500 mA·g^{-1}; (**b**) the discharge/charge profiles of the 1st, 2nd, 3rd, 5th and 10th cycles of the Co$_3$O$_4$@CP electrode; (**c**) Voltage profiles and cycling performance under 100 mA·g^{-1} at a limited capacity of 500 mA·h·g^{-1} based on mass of Co$_3$O$_4$.

The Cyclic Voltammetry (CV) tests of the cell containing the Co$_3$O$_4$@CP electrode were respectively implemented in air and oxygen at a constant scanning frequency of 0.1 mV·s^{-1} between 4.5 and 2.0 V, and the results were shown in Figure 7a. It can be seen that, compared with the CV curves in air, the curves in oxygen indicated higher peak potential and lower peak current for OER, implying that the kinetics of Li$_2$O$_2$ oxidation in oxygen were effectively improved. Furthermore, the CV curve acquired in oxygen has a broadened reduction doublet peak, being at 2.58 and 2.47 V respectively, deriving from the surface-adsorption and solvation mediated growth pathway of Li$_2$O$_2$ [23]. Figure 7b presents electrochemical impedance spectra of the cell with Co$_3$O$_4$@CP electrode initial and after 1st full discharge/charge. It is illustrated that the impedance of the cell increases dramatically after 1st discharge due to the discharge products with poor conductivity generated in the reduction reaction. Unsatisfactorily, there is not obvious decrease in terms of the impedance value after the first charge, indicating that insulated discharge products are not adequately decomposed. Figure 8 reveals the micro morphology of surface of the Co$_3$O$_4$@CP after 1st discharge/charge. By contrast, it can be clearly seen that there are still some discharge products (Li$_2$O$_2$) on the surface of the Co$_3$O$_4$@CP after 1st charge, not being thoroughly decomposed, which is consistent with the characterization results of EIS.
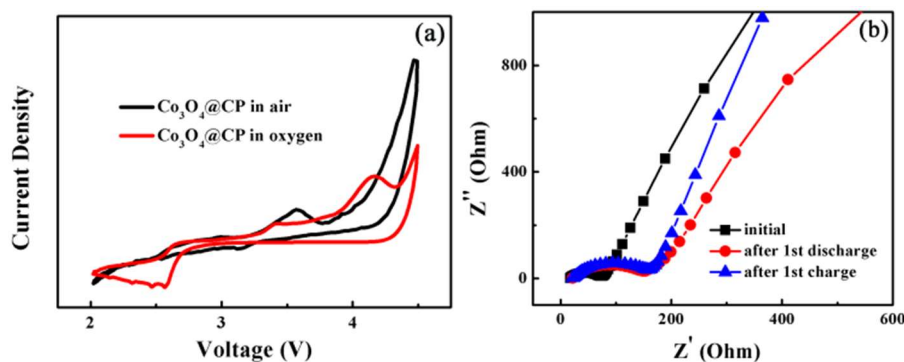
Figure 7. (**a**) CV curves between 2.0 and 4.5 V at 0.1 mV·s^{-1}; (**b**) Electrochemical impedance spectra of Li-O$_2$ batteries with Co$_3$O$_4$@CP electrode initial and after 1st full discharge/charge.
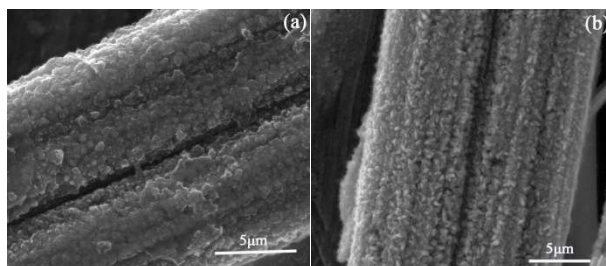
Figure 8. (**a**) and (**b**) SEM of the first discharge/charge, respectively.

4. Conclusions

In order to improve the performance of the lithium-oxygen battery, a Co$_3$O$_4$@CP composite material was fabricated as a cathode using the electrodeposition method. The Co$_3$O$_4$@CP cathode has the following advantages: First, the catalyst Co$_3$O$_4$ was directly deposited on the CP substrate with good conductivity, eliminating the need to add a binder and resulting in a decrease in side reactions. The direct contact between Co$_3$O$_4$ and CP enhances the transport efficiency of electrons in the cathode. Second, the Co$_3$O$_4$@CP composite material has a porous structure, which provides more channels for the diffusion of oxygen and electrolyte, even accommodating more Li$_2$O$_2$ that cannot be decomposed. Third, Co$_3$O$_4$ exists in the form of nanosheets, which supply more catalytic active sites for electrochemical reactions. It is pleasing to note that the cell assembled with the obtained Co$_3$O$_4$@CP electrode showed a discharge specific capacity of 10954.7 mA·h·g^{-1} at 200 mA·g^{-1}, and the voltage profiles of the cell were good under 100 mA·g^{-1} at a limited capacity of 500 mA·h·g^{-1} based on the mass of Co$_3$O$_4$. Thanks to the merits and properties mentioned above, the Co$_3$O$_4$@CP composite can be used as the cathode material in a lithium-oxygen battery.

Supplementary Materials

The supplementary information can be found at https://www.sciepublish.com/index/journals/article/spe/30/id/40 and includes two figures:
Figure S1: EDS of Co$_3$O$_4$@CP.
Figure S2: XRD analysis of Co$_3$O$_4$@CP composites.

Author Contributions

Ethics Statement

Not applicable.

Informed Consent Statement

Not applicable.

Declaration of Competing Interest

The authors declare that they have no known competing financial interests or personal relationships that could have appeared to influence the work reported in this paper.

References

1. Bruce PG, Freunberger SA, Hardwick LJ, Tarascon, J-M. Li-O$_2$ and Li-S batteries with high energy storage. *Nat. Mater.* **2011**, *11*, 19–29.
2. Lu J, Li L, Park JB, Sun YK, Wu F, Amine K. Aprotic and Aqueous Li-O$_2$ Batteries. *Chem. Rev.* **2014**, *114*, 5611–5640.
3. Beattie SD, Manolescu DM, Blair SL. High-Capacity Lithium-Air Cathodes. *J. Electrochem. Soc.* **2009**, *156*, A44–A47.
4. Peng ZQ, Freunberger SA, Chen YH, Bruce PG. A Reversible and Higher-Rate Li-O$_2$ Battery. *Science* **2012**, *337*, 563–566.
5. Li DY, Zhao LL, Xia Q, Wang J, Liu XM, Xu HR, et al. Activating MoS$_2$ Nanoflakes via Sulfur Defect Engineering Wrapped on CNTs for Stable and Efficient Li-O$_2$ Batteries. *Adv. Funct. Mater.* **2022**, *32*, 2108153.
6. Zhou Y, Yin K, Gu QF, Tao L, Li YJ, Tan H, et al. Lewis-Acidic PtIr Multipods Enable High-Performance Li-O$_2$ Batteries. *Angew. Chem. Int. Ed.* **2021**, *60*, 26592–26598.
7. Wang XX, Guan DH, Li F, Li ML, Zheng LJ, Xu JJ. Magnetic and Optical Field Multi-Assisted Li-O$_2$ Batteries with Ultrahigh Energy Efficiency and Cycle Stability. *Adv.Mater.* **2022**, *34*, 2104792.
8. Li F, Li ML, Wang HF, Wang XX, Zheng LJ, Guan DH, et al. Oxygen Vacancy-Mediated Growth of Amorphous Discharge Products toward an Ultrawide Band Light-Assisted Li-O$_2$ Batteries. *Adv.Mater.* **2022**, *34*, 2107826.
9. Huang BW, Li L, He YJ, Liao XZ, He YS, Zhang WM, et al. Enhanced Electrochemical Performance of Nanofibrous CoO/CNF Cathode Catalyst for Li-O$_2$ Batteries. *Electrochim. Acta* **2014**, *137*, 183–189.
10. Zhang Z, Su LW, Yang M, Hu M, Bao J, Wei JP, et al. A composite of Co nanoparticles highly dispersed on N-rich carbon substrates: An efficient electrocatalyst for Li-O$_2$ battery cathodes. *ChemComm* **2014**, *50*, 776–778.
11. Wittmaier D, Canas NA, Biswas I, Friedrich KA. Highly Stable Carbon-Free Ag/Co$_3$O$_4$-Cathodes for Lithium-Air Batteries: Electrochemical and Structural Investigations. *Adv. Energy Mater.* **2015**, *5*, 1500763.
12. Chen YN, Zhang Q, Zhang Z, Zhou XL, Zhong YR, Yang M, et al. Two better than one: cobalt-copper bimetallic yolk-shell nanoparticles supported on graphene as excellent cathode catalysts for Li-O$_2$ batteries. *J. Mater. Chem. A* **2015**, *3*, 17874–17879.
13. Kuang D, Xu L, Liu L, Hu W, Wu Y. Graphene–nickel composites. *Appl. Surf. Sci.* **2013**, *273*, 484–490.
14. Kim DS, Park YJ. Ketjen black/Co$_3$O$_4$ nanocomposite prepared using polydopamine pre-coating layer as a reaction agent: Effective catalyst for air electrodes of Li/air batteries. *J. Alloys Compd.* **2013**, *575*, 319–325.
15. Yoon TH, Park YJ. Polydopamine-assisted carbon nanotubes/Co$_3$O$_4$ composites for rechargeable Li-air batteries. *J. Power Sources* **2013**, *244*, 344–353.
16. Su DW, Dou SX, Wang GX. Single Crystalline Co$_3$O$_4$ Nanocrystals Exposed with Different Crystal Planes for Li-O$_2$ Batteries. *Sci. Rep.* **2014**, *4*, 5767.
17. Pu Z, Liu Q, Asiri AM, Obaid AY, Sun X. One-step electrodeposition fabrication of graphene film-confined WS$_2$ nanoparticles with enhanced electrochemical catalytic activity for hydrogen evolution. *Electrochim. Acta* **2014**, *134*, 8–12.
18. Zhao GY, Lv JX, Xu ZM, Zhang L, Sun KN. Carbon and binder free rechargeable Li-O$_2$ battery cathode with Pt/Co$_3$O$_4$ flake arrays as catalyst. *J. Power Sources* **2014**, *248*, 1270–1274.
19. Lv QL, Zhu Z, Zhao S, Wang LB, Zhao Q, Li FJ, et al. Semiconducting Metal-Organic Polymer Nanosheets for a Photoinvolved Li-O$_2$ Battery under Visible Light. *J. Am. Chem. Soc.* **2021**, *143*, 1941–1947.
20. Li LJ, Liu SY, Manthiram A. Co$_3$O$_4$ nanocrystals coupled with O- and N-doped carbon nanoweb as a synergistic catalyst for hybrid Li-air batteries. *Nano Energy* **2015**, *12*, 852–860.
21. Zhao GY, Xu ZM, Sun KN. Hierarchical porous Co$_3$O$_4$ films as cathode catalysts of rechargeable Li-O$_2$ batteries. *J. Mater. Chem. A* **2013**, *1*, 12862–12867.
22. Zhu J, Ren X, Liu J, Zhang W, Wen Z. Unraveling the Catalytic Mechanism of Co$_3$O$_4$ for the Oxygen Evolution Reaction in a Li–O$_2$ Battery. *ACS Catal.* **2015**, *5*, 73–81.
23. Li F, Wang Y, Bai RS, Wang XX, Li ML, Xu JJ. Resolving the cathode passivation of lithium-oxygen batteries with an amination SiO$_2$/TiO$_2$ functional separator. *J. Power Sources* **2021**, *483*, 229180.